Power dependence of density and current drive efficiency in full LHCD plasmas on TRIAM-1M

K.HANADA, H.Xu[1)], H.IDEI, H.ZUSHI, M.HASEGAWA, K.NAKAMURA, M.SAKAMOTO, K.N.SATO, S.KAWASAKI, H.NAKASHIMA, A.HIGASHIJIMA and K.SASAKI[1)]
Advanced Fusion Research Center, Research Institute for Applied Mechanics, Kyushu University, Kasuga 816-8580, Fukuoka, Japan
E-mail:hanada@triam.kyushu-u.ac.jp
Research Institute for Applied Mechanics, Kyushu Univ., Fukuoka, 861-8580, Japan
1) Interdisciplinary Grad. School of Engineering sciences, Kyushu University, Kasuga 816-8580, Fukuoka, Japan

Abstract

Full lower hybrid current drive (LHCD) plasmas on TRIAM-1M have been investigated in the wide ranges of line-averaged electron density, $\bar{n}_e$ =0.1-4.7$\times 10^{19}$m^{-3}, plasma current, I_P=15-100kA, and injected power, P_{LH}=0.003-0.2MW. Strong gas-puff makes a termination of the discharge in high density region, where the density is still much lower than the limit predicted by wave propagation characteristics. The achieved $\bar{n}_e$ and the current drive efficiency, η_{CD}, have a significant relation to P_{LH}, and their power dependences are close to the one predicted by a model derived from the balance between the energy confinement, τ_E, and η_{CD} of the LHCD scalings. This density limit depends on the injected P_{LH}. This limit will appear in full CD discharges, including ECCD, NBCD, and bootstrap current and it wanes with the increase of the portion of the ohmic heating power.

1. Introduction

To obtain the steady state full current drive (CD) discharge in high density region as possible is one of the key issues for the realization of cost-effective fusion power plant. Many kinds of current drive tool were nominated and examined in various devices. Lower hybrid current drive (LHCD) is a powerful tool to generate and maintain the plasma current non-inductively and the full LHCD plasmas have been studied in many tokamak devices [1-4]. Recently LHCD in the high density region, that is in ITER relevant region (~1x10^{20}m^{-3}) was reported in FTU [5]. A 5 h discharge was obtained in very low density region on TRIAM-1M [6, 7]. A steady-state full LHCD discharge in intermediate density was achieved on Tore Supra and total injected energy reached up to beyond 1GJ [8].

High power will be required to obtain the high density plasma, however in steady state condition, the balance between injected heating power and removable power from plasma facing components (PFC) is significant [7, 8] and the injected power is limited by plasma wall interaction (PWI), including production of impurity and erosion of material. Therefore the available power is limited by the cooling capability of the device. The wave propagation capability such as the accessibility condition of lower hybrid wave (LHW) sometimes plays an essential role in the achievement of the high density discharge. As for the accessibility condition, high toroidal magnetic field plays an essential role in the wave propagation to the plasma center. TRIAM-1M has 16 superconducting toroidal coils, which is able to generate the torodal magnetic field up to 8T at the plasma center in steady sate and three kinds of current drive sources in frequency with 2.45, 8.2, 170 GHz are available. Therefore TRIAM-1M is suitable to execute the experiments to try to obtain high density

steady state LHCD discharges.

On TRIAM-1M, full LHCD plasmas were obtained in the wide ranges of line-averaged electron density, $\bar{n}_e$ =0.1-4.7 × $10^{19}$$m^{-3}$, plasma current, I_P=15-100kA, and injected power, P_{LH}=0.003-0.2MW. The power dependence of achieved density and current drive efficiency are reported and a simple model is introduced to explain the tendency. In section 2, the experimental apparatus is introduced and the experimental results are summarized in the section 3. The simple model is proposed in the section 4 and the conclusion is described in the section 5.

2. Experimental apparatus

TRIAM-1M (R=0.84m, a x b=0.12m x 0.18m) is a small size high magnetic field tokamak with 16 superconducting toroidal magnetic field coils made of Nb_3Sn, which produces the toroidal magnetic field, B_T, up to 8T in steady state. A 2.45GHz LHCD system, which has a klystron (2.45GHz, maximum power = 50kW), two 8.2 GHz LHCD systems, which have 8 klystrons (8.2GHz, maximum power = 25kW per a klystron), and an electron cyclotron heating (ECH) system, which has a gyrotron (170 GHz, maximum power = 200kW) are installed on TRIAM-1M as additional heating sources. Experiments described in this paper are carried out by use of the combination of two 8.2 GHz LHCD systems and a 2.45GHz one.

As for the 8.2 GHz LHCD systems, source microwave generated by a DIO has been divided by 2 branches at first. One branch is source microwave for a system and another one is for another system. Each source microwave has been divided by 8 branches and transmitted through a phase shifter driven by a motor and an attenuator in each branch. Microwave amplified by an 8.2 GHz klystron up to 25 kW has been transmitted by water-cooled waveguides with rectangle cross-section. High power microwave has been divided by 2 branches. One branch has a phase shifter for high power microwave. High power microwave in each system has been injected into plasma through an 8x2 grill type launcher from low field side and LHW can be excited in the plasma. The phase velocity of the excited LHW can be varied by the phase difference in the adjacent waveguide of the launcher, which is controlled by the phase shifter in each transmitted line described above. One system has the capability to change the power during the discharge and change the phase velocity of LHW shot by shot. Another system has the capability to control the phase velocity of LHW

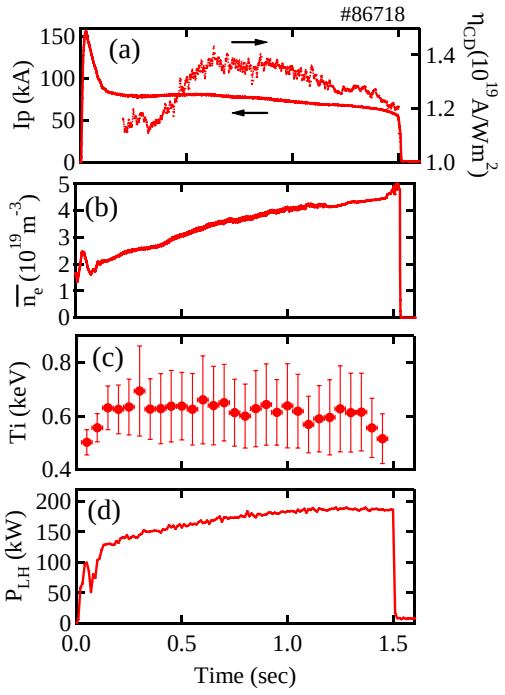

Fig.1 Time evolution of plasma current, I_P, (solid line) and current drive efficiency, η_{CD}, (dotted line) (a), line averaged electron density, $\bar{n}_e$ (b), ion temperature, T_i (c), and LHW power, P_{LH} (c).

during a discharge with 10 degree per a second as well as the power. When the reflected power is over a certain level, the power of microwave is stopped immediately to avoid the break of vacuum windows, which is made of thin sapphire cooled by water in each transmitted line.

As for the 2.45 GHz LHCD system, source microwave is generated by a crystal oscillator. Microwave amplified by a 2.45 GHz klystron up to 50 kW has been transmitted by water-cooled waveguides with rectangle cross-section. High power microwave has been divided by 4 branches. One branch has a phase shifter for high power microwave. High power microwave in each system has been injected into plasma through a 4x1 grill type launcher from low field side and LHW can be excited in the plasma.

3. Experimental results

The strong gas-puffing was executed to obtain the high density full LHCD plasmas and the achieved typical waveforms of the high density discharge are shown in Fig.1. Although the net injected power is about 0.2MW, the generated powers at the klystrons are the almost maximum of the systems. A part of the power was lost in waveguides (15-20%) and a part was reflected at the plasma surface (10-20%). The value of $\bar{n}_e$ was increasing with P_{LH} from 0.2 to 1 s. The values of I_P and η_{CD}, gradually decreases for 1-1.5 s under the constant P_{LH}. The maximum of the achieved density is 4.7×10^{19} m^{-3}, which is far from the predicted density limit ($3x10^{20}m^{-3}$) by Sverdrup and Wegrowe [9] models, which are

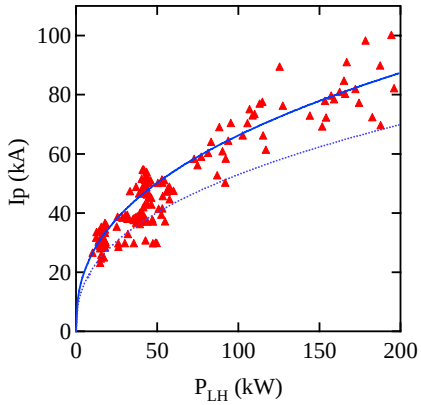

Fig.2 The achieved plasma current, I_P, during full LHCD are plotted as the function of injected power. The solid and dotted lines show the fitting value.

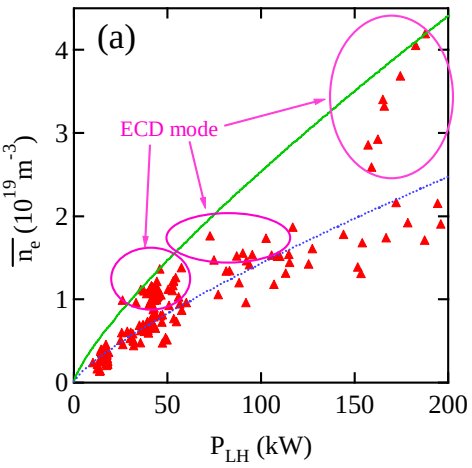

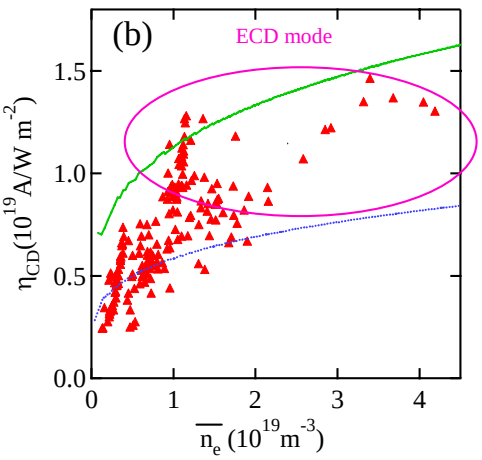

Fig.3 (a) The densities at the time of the peak plasma current during full LHCD are plotted as the function of injected power. The solid (L mode) and dotted (L mode X 0.8) lines show the calculated value based on the model in the section 4. Ellipses show the regions of the ECD plasma. (b): The current drive efficiencies as the function of electron density. The ellipses show the region of ECD plasma.

based on the wave propagation characteristics as described in section 4. This indicates that the density in full LHCD plasmas on TRIAM-1M is not restricted by the wave propagation characteristics. However any discharges with higher density (>4.7×10^{19} m^{-3}) can not be obtained. Before the termination of the discharge, $\bar{n}_e$ was increasing and the reduction of I_P, η_{CD}, and ion temperature, T_i was observed. Finally the plasma current went to zero. At the final phase of the discharge (before 100ms from the termination), strong impurity incorporation was happen. This shows the present LHW power (~0.2MW) is close to the limitation based on PWI effect such as impurity incorporation to the plasma. It should be noted that although the peak value of $\bar{n}_e$ in this discharge is tentatively about 4.7×10^{19} m^{-3}, the maximum of $\bar{n}_e$ in steady state is 4.3×10^{19} m^{-3}.

The power dependence of plasma current during full LHCD plasmas is plotted in Fig. 2. In the range of less than 20kW, the plasma is sustained by 2.45GHz LHCD and the other is the data obtained by 8.2GHz LHCD systems. The solid line in Fig. 2 shows the fitting curve of the data for the ECD mode and it is expressed by

$$I_P[kA] = 10.5(P_{LH}[kW])^{0.4} \qquad (1),$$

and the dotted one shows the fitting curve for non ECD mode and it is expressed by

$$I_P[kA] = 8.4(P_{LH}[kW])^{0.4} \qquad (2).$$

The power dependence of density was also investigated in full LHCD plasma as shown in Fig. 3(a) and the achieved $\bar{n}_e$ depends on P_{LH}. The solid line shows the power dependence of $\bar{n}_e$ derived from the equations (3) - (5) as described in the section 4. With the increase of P_{LH}, the achieved $\bar{n}_e$ The dependence is similar to the data except enhanced current drive (ECD) mode [10], where τ_E , η_{CD} are better than no ECD discharge.

On TRIAM-1M, the current drive efficiency, η_{CD}, increases with the density as shown in Fig. 3(b). This is not predicted by the Fisch's LHCD theory [11]. The equations (1), (2), and (4) lead to the density dependence of η_{CD} and the result is shown as a curve in Fig.3(b). In ECD mode, strong density dependence [12] is observed as shown in Fig. 3(b).

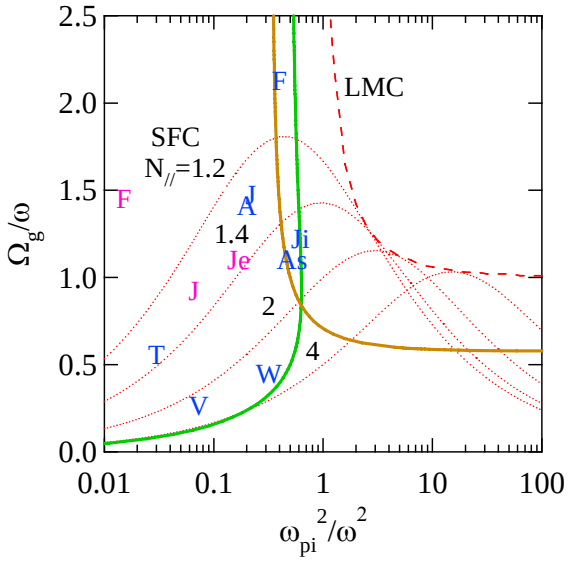

Fig.4 Density limit of LHCD plasmas on various devices. Green and brown lines show the limits predicted by Sverdrup and Wegrowe models, respectively. Blue texts (J:JT-60, F;FT, A:Alcator-C, Ji:JIPP-T2, W;WT-3, V:Versator-2, As:ASDEX, T;TRIAM-1M) correspond to the data of density limit and red ones (J:JT-60, Je;JET, F;FTU) show the high current and density LHCD data.

4. The model for the density limit

Several models to explain the density limit of LHCD plasmas were proposed [9]. The proposed density limits and the data in various devices are plotted in Fig. 4. Although the data from various devices are not so far from the curve proposed by Sverdrup's model [9], the data from TRIAM-1M is far from proposed density limit models and it is also far from linear mode conversion point (LMC). Moreover it is close slow-fast mode conversion (SFC) point of $N_{//}$=1.4, which is lower than

the peak value of $N_{//}$ (~1.8) of the excited LHW. This clearly shows that the accessibility condition does not play an essential role in the density limit as shown in Fig. 1.

To explain the density limit observed on TRIAM-1M, a simple model is proposed here. According to the proposed scaling for the LHCD [12] and bootstrap current, the plasma current, I_P, can be expressed by

$$I_P(A) = \frac{0.012}{5+Z_{eff}}\langle T_e\rangle \frac{P_{LH}}{1.34\langle n_e\rangle R} + 54\left(\frac{a}{R}\right)^{1/2}\langle n_e\rangle\langle T_e\rangle\frac{R}{B_T} + 0.95\times10^{-4}\langle T_e\rangle^{3/2}\frac{P_{OH}}{Z_{eff}I_P}\pi a^2 \quad (3).$$

The first term expresses the LHCD effect based on the LHCD scaling [12] and the second one is derived from the bootstrap current and the third one show the OH current. This equation is plotted at the given I_P and P_{LH} in Fig.5, where Z_{eff}=3 is assumed. On the other hand, $\langle n_e\rangle$ depends on $\langle T_e\rangle$ owing to the energy balance equation,

$$3\langle n_e\rangle\langle T_e\rangle V_{plasma} = \tau_E P_{LH} \quad (4),$$

where V_{plasma} and τ_E are plasma volume and the energy confinement time, respectively. As we assume the parabolic density profile, the relation,

$$\bar{n}_e = 1.34 < n_e > \quad (5),$$

is used in the equations.

The L-mode scaling [12] is used as τ_E in Fig. 5. The right side term of the Eq. (4) at the given I_P and P_{LH} is also plotted as the red lines in Fig. 5. And the left term of the Eq. (4) substituted by the Eq. (3) is also plotted as the blue and green curves in Fig. 5. The intersection point shows the realized $\langle n_e\rangle$ and $\langle T_e\rangle$ based on the Eq. (4). It should be noted that the calculated $\langle n_e\rangle$ does not depend on I_P as shown by the points A and B in Fig. 5, because the dependence of I_P is almost canceled in Eqs. (1) and (2). When I_P is 80kA in full CD discharge, the intersection point (A) is $\langle n_e\rangle = 2.2\times10^{19}m^{-3}$, $\langle T_e\rangle = 0.65keV$. When I_P is 60kA, the intersection point (B) moves to $\langle n_e\rangle = 2.2\times10^{19}m^{-3}$, $\langle T_e\rangle = 0.5keV$. On TRIAM-1M, the portion of bootstrap current is not so much. When the part of power is used for the OH current, the situation is drastically changed. The current drive efficiency of OH discharge is significantly better than the other CD methods, and current drive efficiency is proportional to $\langle T_e\rangle^{3/2}$. The results are shown in Fig. 5. The value of 10% power is used for the OH current, the achievable density is significantly higher than full CD case (see the intersection points C and D). The typical difference appears in the value of $\langle n_e\rangle$, because the value of $\langle n_e\rangle$ is shifted when I_P changes.

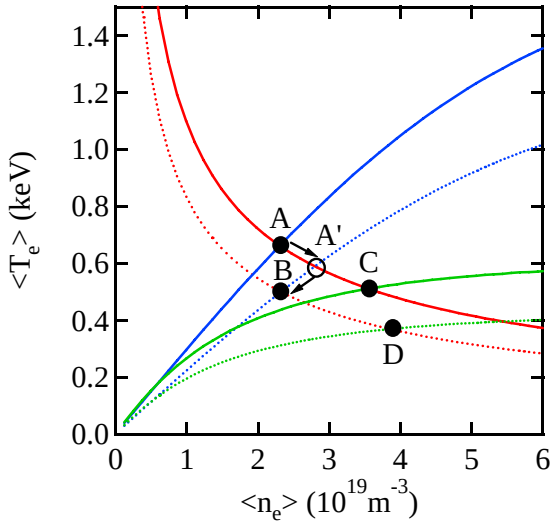

Fig. 5 An example of the balance between the L mode confinement and current drive scalings. Point A and B show the intersection points in the cases of Ip=80 and 60kA at 0.2MW in full LHCD discharge, respectively. The blue (full CD) and green (90% CD) lines are derived form the equation (2) (solid:80kA, dotted:60kA). Point C and D show the intersection points in the cases of Ip=80 and 60kA at 0.2MW in 90% LHCD discharge, respectively. Point A' shows the tentative state in the plasma termination phase.

According to this model, the value of $\langle n_e \rangle$ is derived as the function of P_{LH} as shown in Fig. 3(a). The relation between $\langle n_e \rangle$ and P_{LH} is able to be expressed by the model.

Based on this model, the plasma termination in full CD discharges shown in Fig. 1 can be explained as follows. The density is determined by the intersection point as shown in Fig. 5 for a given P_{LH} (see point A). The strong gas-puffing will tend to make $\langle n_e \rangle$ increase and to make $\langle T_e \rangle$ decrease along the line derived from the confinement scaling (see point A'). Therefore the point seems to move along the arrow in Fig. 5. Then I_P will go down, because of the reduction of η_{CD}, which is proportional to $\langle T_e \rangle$. The value of τ_E is also reduced by the decreasing of I_P. As the result, $\langle n_e \rangle$ comes back to the previous value (see point B), although I_P and $\langle T_e \rangle$ are reduced. This process may work gradually for 1-1.4sec in Fig. 1, because $\langle n_e \rangle$ is kept constant. However the acceleration of this process leads to the rapid deduction of I_P and $\langle T_e \rangle$ and finally the plasma termination takes place as shown in Fig.1. This clearly shows in Fig. 6. When we want to increase $\langle n_e \rangle$ in full CD discharges, rapid current reduction takes place at a certain density, which is determined by the injected power and the scalings of the plasma confinement and the current drive efficiency. When the slight OH power is injected, the dependence of I_P on $\langle n_e \rangle$ is significantly changed. This is the reason to obtain the OH + CD discharge with various density. This tendency is the same in other non-inductive current drive method including NBCD, ECCD and bootstrap current, because the current drive efficiency of them is almost proportional to $\langle T_e \rangle$ as the same of the LHCD scaling.

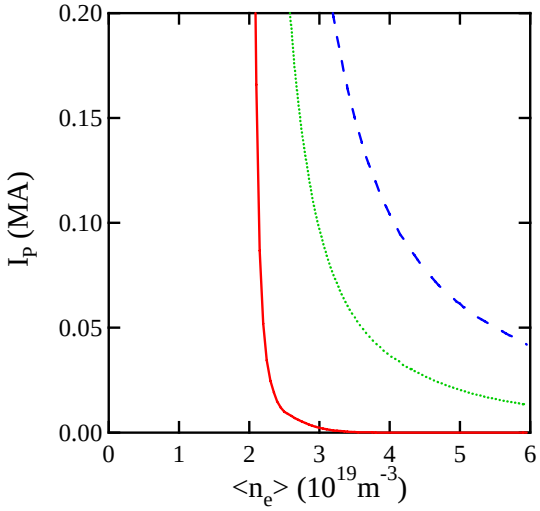

Fig. 6 The relation between $\langle n_e \rangle$ and I_P based on the model is plotted. Solid line shows the case of full CD and the dotted one shows the case of 90% CD , and the dashed one shows the case of 80% CD. Total injected power is 0.2MW and Z_{eff}=3.

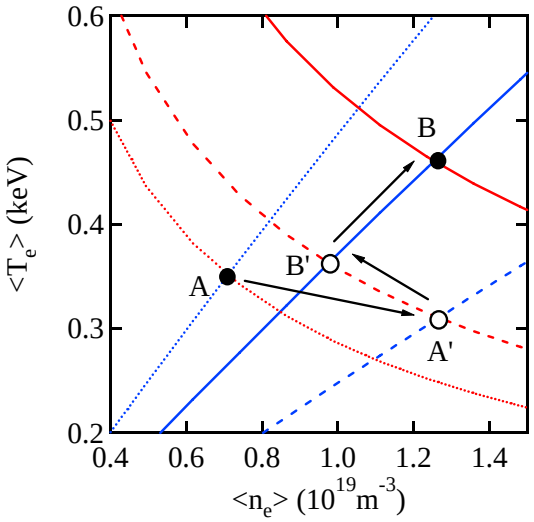

Fig. 7 The red solid and the red dashed lines show the L mode scalings at I_P=0.06MA and 0.04MA, respectively. The red dotted line shows the L mode scaling at H=0.8, I_P=0.04MA, where H means the H factor. The blue solid, and dashed lines show the twice of the LHCD scaling at I_P=0.06MA, 0.04MA. The blue dotted line shows the LHCD scaling at I_P=0.04MA. All calculations are executed at P_{LH}=0.06MW, Z_{eff}=3.

In the ECD mode discharge, the higher η_{CD} can be observed as shown in Fig. 3(b). Surely the confinement time in ECD mode is better than that in the non ECD ones and the

current drive efficiency is also enhanced by 2 [13]. This can be expressed by the model as shown in Fig. 7. At first, the plasma parameters show the intersection point between the L mode scaling at H=0.8 and the full CD scaling (see point A), where H means the H factor. The energy confinement and the current drive scalings are improved simultaneously and the point moves to A' in Fig. 7. After that, the plasma current increases by 1.5 times due to the improved drive efficiency (see point B'). The energy confinement is also improved by the increased plasma current. Finally the point is located on the point B. This is the reason of the current, the density and the temperature increment in ECD mode.

5. Conclusion

Full lower hybrid current drive (LHCD) plasmas on TRIAM-1M have been investigated in the wide ranges of line-averaged electron density, $\bar{n}_e$ =0.1-4.7$\times 10^{19}$m^{-3}, plasma current, I_P=15-100kA, and injected power, P_{LH}=0.003-0.2MW. The power dependences of density and plasma current in full LHCD discharges are obtained. Especially the density in full LHCD plasma is not limited by the wave propagation condition, but by the balance between the plasma confinement and the current drive efficiency. The model can obtain the dependence of current drive efficiency on density, which is not predicted by the current drive theory. The model does not have the contradiction with the observation of the transition to the enhanced current drive mode on TRIAM-1M.

6. Acknowledgement

This work was partially performed under the framework of joint-use research at RIAM Kyushu University and the bi-directional collaboration organized by NIFS. This work is partially supported by a Grant-in-Aid for Scientific Research from Ministry of Education, Science and Culture of Japan.

7. References

[1] R.Yoshino and JT-60Team:Plasma Phys. and Contrl. Fusion **29** No.10A(1987) 1377.
[2] Y.Ikeda et al., in Proc. 15th Inter. Conf. on plasma physics and controlled nuclear fusion research, (Seville, 1994) **1** 415.
[3] JET team in Proc. 15th Inter. Conf. on plasma physics and controlled nuclear fusion research, (Seville, 1994) **1** 423.
[4] M.Porkolab, J.J.Schuss, et al., Phys. Rev. Lett. **53** (1984) 450.
[5] G. Granucci et al., Fusion Science &Tech. **45** (2004) 387, V.Pericoli-Ridolfini et al., Phys. Rev. Lett. **82** (1999) 93.
[6] H.Zushi et al., Nuclear Fusion **45** (2005) S142-S156.
[7] K.Hanada, et al., Fusion Engineering and design **81** (2006) 2257-2265.
[8] J. Jacquinot, Nucl. Fusion **45** (2005) S118-S131.
[9] L.H.Sverdrup et al., Phys. Rev. Lett., Vol.59, No.11, pp.1197-1200 (1987).
[10]K.Hanada, Nulc. Fusion, Vol.41, No.11, pp1539-1542 (2001).
[11]N.J.Fisch, Phys. Rev. Lett. 41 (1978) 873, N.J.Fisch, Review of Modern Physics **59** (1987) 175.
[12] ITER Physics Basis, Nulc. Fusion, Vol.39, No12 (1999).
[13] H.Zushi et al., Nuclear Fusion **41** (2001) 1483-1493.